PROCEEDINGS OF SPIE

SPIEDigitalLibrary.org/conference-proceedings-of-spie

Band structure calculation of dilute-As GaNAs by first principle

Xiao-Hang Li
Hua Tong
Hongping Zhao
Nelson Tansu

SPIE.

Band Structure Calculation of dilute-As GaNAs by First Principle

Xiao-Hang Li [+], Hua Tong, Hongping Zhao, and Nelson Tansu [±]
Center for Optical Technologies, Department of Electrical and Computer Engineering,
Lehigh University, Bethlehem, PA 18015
[+]Email: Li@Lehigh.Edu, [±]Email: Tansu@Lehigh.Edu

ABSTRACT

We present the band structure calculation of dilute-As GaNAs alloys (from 0% to 6.25% As) by employing the density-functional theory that adopts the local density approximation. Our studies indicate that the GaNAs shows a direct bandgap property. A small incorporation of As into the GaN alloy leads to the a significant decrease in the energy gap, which allows direct band gap transition covering from 3.47 eV (0% As) down to 1.93eV (6.25% As). The finding implies the dilute-As GaNAs alloy as an excellent candidate for the active material for optoelectronics that covers the entire visible spectral regime. The carrier effective masses of dilute-As GaNAs alloys are also presented.

Keywords: dilute-As GaNAs, first principle, visible spectrum, effective mass.

1. INTRODUCTION

The III-Nitride semiconductors have many interesting and useful properties such as having direct band gaps at the gamma point in the Brillouin Zone. The energy gaps of III-Nitride semiconductor covers the whole visible spectrum as well as the ultraviolet and infrared spectrum, thus this material system plays a very important role for light-emitting diodes (LEDs) and laser diodes. The InGaN alloy has been implemented for nitride-based light-emitting diodes in solid state lighting [1-12], and the properties of the $In_xGa_{1-x}N$ alloy have been investigated vigorously. For GaNAs ternaries, significant studies have also been carried out on understanding the electronic structure, epitaxial growth, device fabrication and engineering of dilute-nitride GaNAs (up to 5% N) for achieving the near-infrared quantum well lasers [13-24]. In contrast to the development in dilute-nitride GaNAs semiconductor, very limited experimental work [25] and new device concepts [26, 27] based on dilute-As GaNAs alloy. The studies of the basic material physics and properties of dilute-As GaNAs alloy are very lacking, thus the accurate understand of the band structure of this alloy are important to provide guidance and insight for device physics of nanostructures employing this alloy. The important parameters such as the band gap and carrier effective mass near the gamma point of the Brillouin zone (BZ) of dilute-As GaNAs alloy have fundamental impacts on the development and implementation of this alloy into advanced device applications.

In this work, we present a first principle study based on Density Functional Theory (DFT) to compute accurate band structure and band properties of dilute-As GaNAs ternary alloy with different As concentrations from 0% up to 6.25%. First of all, we discuss the first principle calculation formation for the dilute-As GaNAs which includes the introduction to the Density-Functional Theory (DFT), the scissor operator, the supercell approach, as well as the details of the calculation steps shown in a flow chart. Then, we will present the band structure of the dilute-As GaNAs, and the band gap extracted from the band structure. The material properties such as the effective masses of the electrons, heavy holes as well as the light holes of the dilute-As GaNAs alloy are presented in this study.

2. FIRST PRINCIPLE CALCULATION FORMULATION

The first principle calculation is a very important technique to explore the electronic properties of novel materials with unfamiliar band and material properties. The use of DFT technique solves the Schrödinger's equation of the electron

Physics and Simulation of Optoelectronic Devices XVIII, edited by
Bernd Witzigmann, Fritz Henneberger, Yasuhiko Arakawa, Marek Osinski, Proc. of SPIE
Vol. 7597, 75970H · © 2010 SPIE · CCC code: 0277-786X/10/$18 · doi: 10.1117/12.842931

in a specific crystal structure by virtue of five physics basic constants, m_e, e, h, c, k_B as shown below. The Schrödinger's equation of an electron can be written as

$$(H_e + H_N + H_{e-N})\Psi(r,R) = E^H \Psi(r,R) \quad (1),$$

where the total Hamiltonian on the left hand side has three components:

Electron: $$H_e = T_e(r) + V_e(r) = -\sum_i \frac{\hbar^2}{2m}\nabla {r_i}^2 + \frac{1}{2}\sum_{i,i'} \frac{e^2}{\left|r_i - r_i'\right|} \quad (2),$$

Nuclei: $$H_N(R) = T_N(R) + V_N(R) = -\sum_j \frac{\hbar^2}{2M_j}\nabla {R_j}^2 + \frac{1}{2}\sum_{j,j'} V_N(R_j - R_j') \quad (3),$$

Electron-Nuclei: $$H_{e-N}(r,R) = -\sum_{i,j} V_{e-N}(r_i - R_j) \quad (4).$$

However, due to the well-known complexity of many-body computation, the first principle calculation over numerous electrons in any crystal structure is computationally unattainable. This problem has been well solved by the use of Density-Functional Theory (DFT) [28], which simplifies Schrödinger's equation into Kohn-Sham equation as below,

Kohn-Sham Equation: $$\{-\frac{\hbar^2}{2m}\nabla^2 + V_{KS}[\rho(r)]\}\psi_i(r) = E_i\psi_i(r) \quad (5).$$

In addition to the kinetic energy term $-\frac{\hbar^2}{2m}\nabla^2$, the total Hamiltonian on the left hand side has a Kohn-Sham potential, which can be described as follow:

Kohn-Sham Potential: $$V_{KS}[\rho(r)] = v(r) + \int \frac{\rho(r')}{\left|r - r'\right|}dr' + V_{XC}[\rho(r)] \quad (6).$$

The Kohn-Sham potential contains an exchange-correlation potential $V_{XC}[\rho(r)]$, which includes all the interaction between electrons and nuclei. The exchange-correlation potential $V_{XC}[\rho(r)]$ can be expressed in several approximation forms, and the local density approximation (LDA) has been used in this study. However, the density-functional theory has an underestimation on the conduction band energy levels. A well-known technique to solve this problem is by applying the "scissor operator" to shift all the conduction bands up relative to all the valence bands [29]. This method supplies a satisfied accuracy for the band gap calculation while significantly decreases the calculation expense compared with other methods like GW quasi-particle approximation.

In the impurity incorporation calculation, the supercell approach is most commonly used [30]. In constructing the supercell, the impurity is surrounded by a number of host atoms and the whole system repeats periodically in space [31-34]. In our study, the dilute-As GaNAs supercell consists of a number of GaN primitive cells and one As atom substitutes one N atom artificially. As an example, the $GaN_{0.9375}As_{0.0625}$ alloy is shown as below, which is represented by a supercell that contains eight GaN primitive cells with 32 atoms where one As atom replaces the position of one N atom. In this study, the numbers of atoms in supercells are 96, 72, 48, 32, which correspond to the As concentrations of 2.08%,

2.78%, 4.16% and 6.25%, respectively. Meanwhile we have calculated pure GaN that has been well studied, which correspond to 0% As concentration. These sets of As concentrations represents dilute-As GaNAs with As-concentration ranging from 0% up to 6.25%.

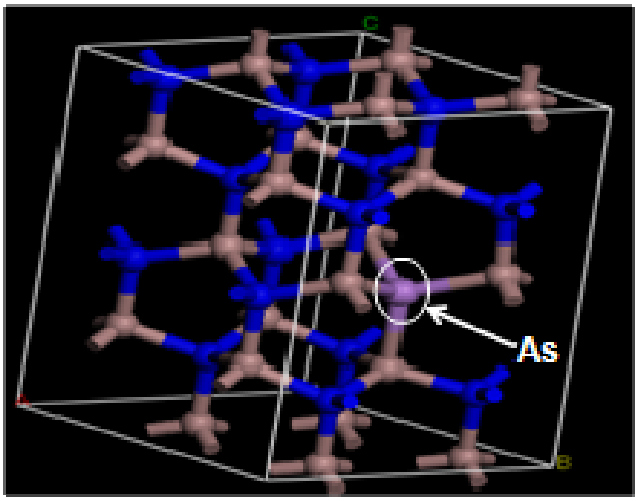

***Figure 1**: $GaN_{0.9375}As_{0.0625}$ supercell consists of 8 GaN primitive cells and one As-atom substituting one N-atom.*

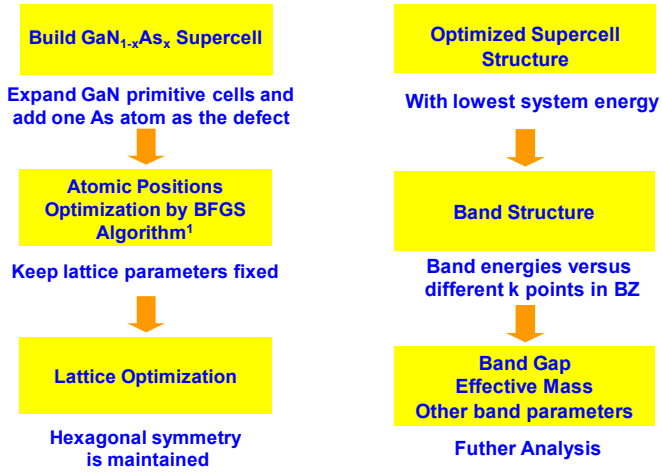

***Figure 2**: Flow chart of computational steps in first principle calculation of dilute-As GaNAs alloy.*

After the supercell was constructed, the structure was optimized by numerical minimization of the total energy self-consistently in two steps. The first step optimized the atomic positions while keeping the lattice parameters fixed by using the Broyden-Fletcher-Goldfarb-Shanno minimization (BFGS) algorithm [35]. The second step initialized with the relaxed coordinates from the first step, and then the atomic coordinates and lattice parameters were optimized synchronously with the hexagonal symmetry maintained. After the optimized structure with lowest system energy was achieved, the band structure of dilute-As GaNAs for a particular composition was computed by using the Density-Functional Theory that adopted local density approximation, where the well-established Perdew-Wang 92 version of LDA was used. For pseudopotentials, the Fritz-Haber-Institute (FHI) form that explicitly included the semicore d-electron effect of group III atoms in the valence band was used in order to obtain reliable band structures. A plane wave basis was employed to expand the wave functions with the plane wave cutoff energy of 700eV, which was tested to be

sufficient for the convergence and accuracy of relevant properties. The calculation routine was along high-symmetrical k-points in the Brillouin zone (BZ). The Monkhorst-Pack grid was used for the k-point summation. The spin-orbit coupling effect was excluded whose influence on wide bandgap III-Nitride semiconductors could be neglected. For convenience, the energy level of the valence band top at gamma point was set to be zero in plotting the band structure. The flow chart of the calculation steps are briefly illustrated in figure 2.

3. BAND PARAMETERS OF DILUTE-AS GANAS ALLOY

After the band energies of dilute-As GaNAs over different k point were obtained from first principle, the band structure was plotted for the band energy levels versus high-symmetrical k-point routines in the Brillouin zone. The band structures of GaN and dilute-As GaNAs alloys were shown in figure 3. The horizontal axis represents different k points in the Brillouin zone and the vertical axis represented the energy levels of the bands. In our study, the band structures of dilute-As GaNAs with different GaN concentrations were found to be similar with each other, and the red circle indicates that all of them have direct band gaps, which is perfect for the direct transition due to the conservation of momentum and energy. The band gaps and the corresponding wavelength are plotted in figure 4, showing a full coverage over the visible spectrum from 1.9 eV up to 3.5 eV.

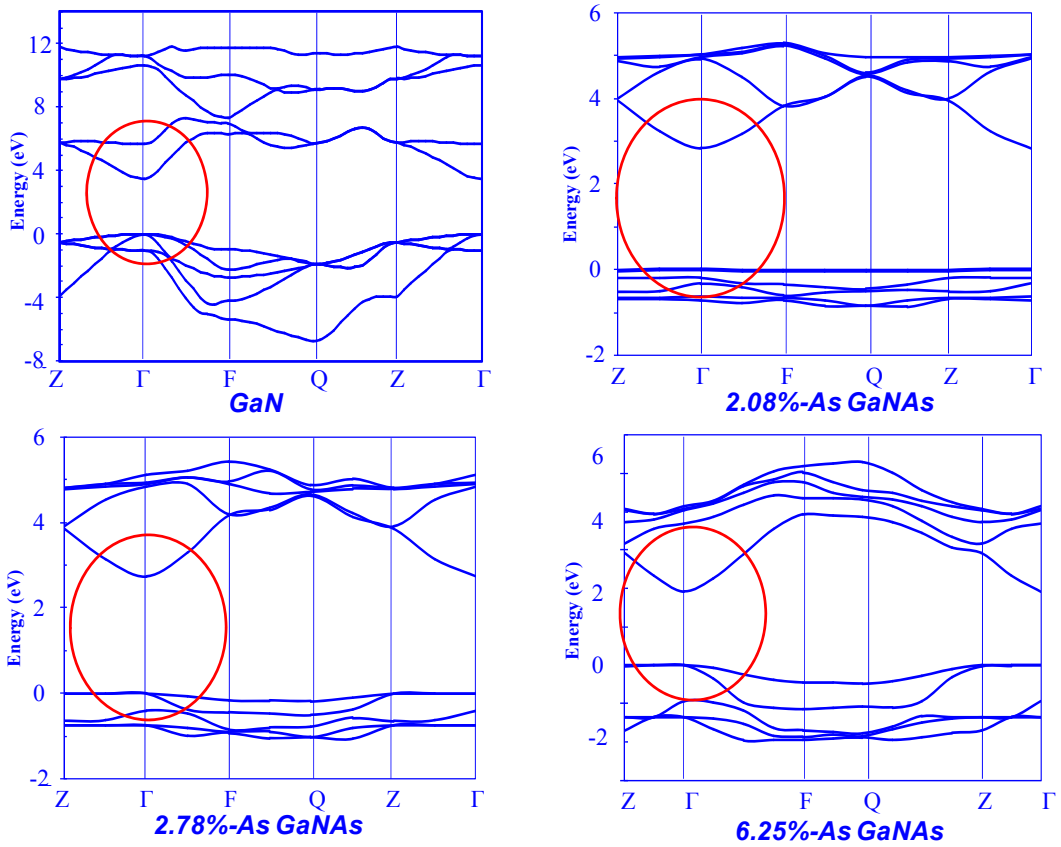

***Figure 3**: Band structures of dilute-As GaNAs with varying As contents. The band structures were shown for GaNAs with As-contents of a) 0%, b) 2.08%, c) 2.78%, and d) 6.25%.*

The energy band gap from our study show good agreement with the experimental values obtained from MOCVD-grown dilute-As GaNAs reported by Wu *et al* [25], as plotted in figure 5. The comparison results indicate a good agreement for both theory and experiment at lower As concentration (<3.5%), however a large discrepancy at higher As concentration (>3.5%) is observed. This disagreement at higher As-content (>3.5%) could result from the finding that the substitutional fraction of As atom over N atom are relatively constant at 90% for low As-content (<3.5%), but the substitutional fraction of As atom over N atom drops rapidly for As-content above 3.5% for MOCVD-grown dilute-As

GaNAs alloy [25]. The incompleteness of As incorporation into GaN at higher As concentration reduces the effect of decreasing Eg with increasing As content. This discrepancy may be relieved or solved by optimizing MOCVD epitaxy.

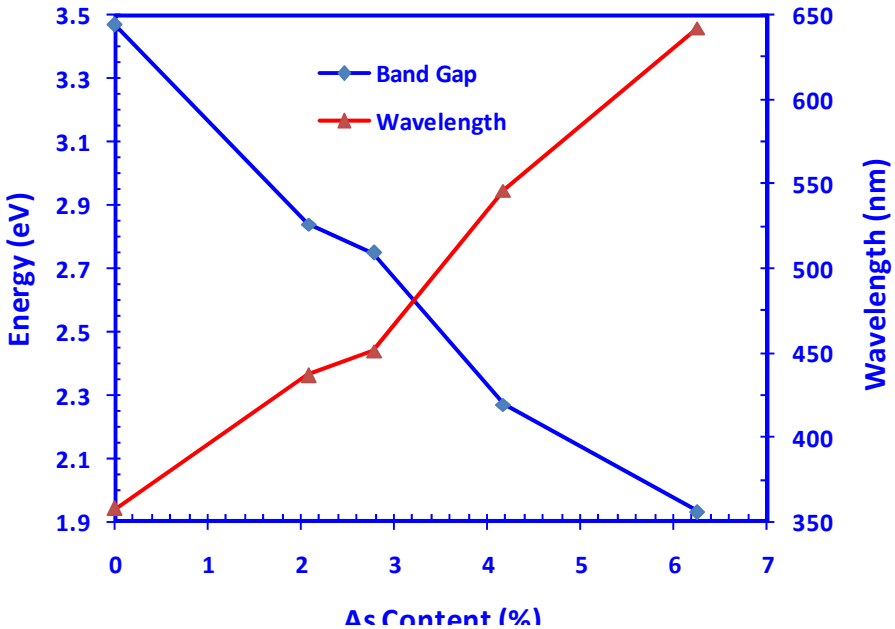

***Figure 4**: Band gaps and corresponding wavelength of dilute-As GaNAs from first principle calculation*

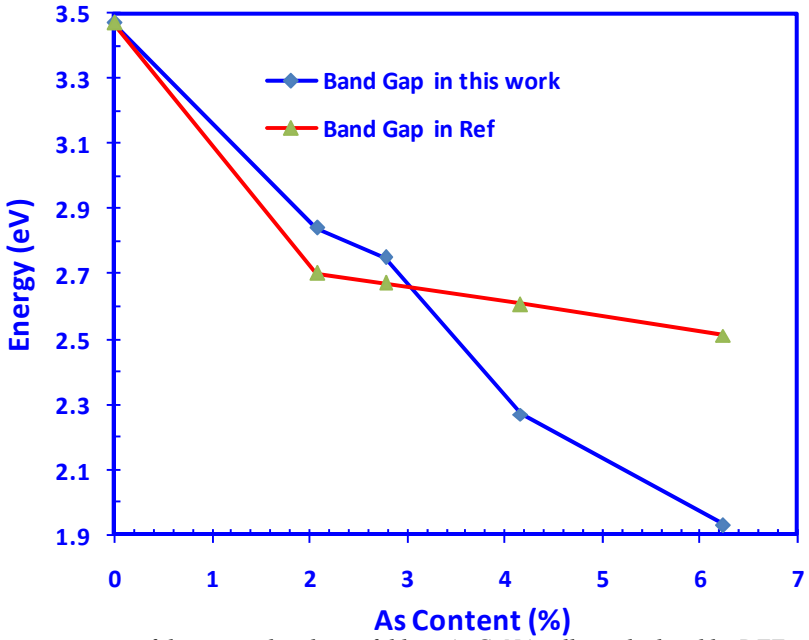

***Figure 5**: The comparison of the energy bandgap of dilute-As GaNAs alloy calculated by DFT and experimental works (by Wu, et. al. [25]).*

The effective masses of the electron, the heavy hole and the light hole of the dilute-As GaNAs alloy were calculated from the band structure. To verify the model we used, the effective masses of carriers of GaN from our study were compared with the values reported by Vurgaftman *et. al.* [36], which show good agreement (Table I). The average effective masses of the carriers of dilute-As GaNAs are shown in figure 6. The electron effective masses of dilute-As

GaNAs are relatively constant as a function of As-contents. However, the incorporation of small amount of As into the GaNAs alloy appears to impact the heavy hole masses significantly.

Materials	Electron	Electron	HH	HH	LH	LH	SOH	SOH
unit (m_0)	$m\parallel$	$m^{\perp}$	$m\parallel$	$m^{\perp}$	$m\parallel$	$m^{\perp}$	$m\parallel$	$m^{\perp}$
0%-As GaN[1]	0.20	0.20	1.89	2.00	1.89	0.14	0.14	2.27
0%-As GaN	0.18	0.18	2.07	2.32	2.07	0.18	0.15	1.55

***Table I**: Comparison of the effective masses of the carriers in GaN calculated from our model, and the results are compared with the values from Vurgaftman et al [36].Note that: HH=heavy hole, LH=light hole, SOH=split-off hole.*

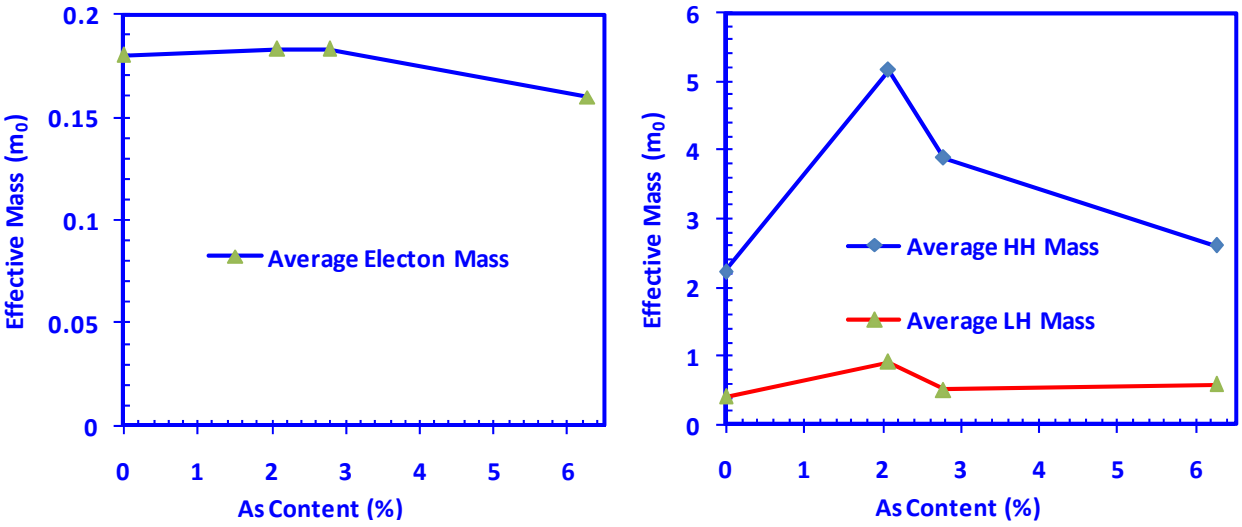

***Figure 6**:The average effective masses of the carriers for dilute-As GaNAs alloy. Note that: HH=heavy hole, LH=light hole.*

4. SUMMARY

In summary, we present the first principle calculation of the electronic properties of dilute-As GaNAs with As content from 0% to 6.25% as a rarely-studied material. The band structures for the GaNAs up to 6.25% As-content indicate direct bandgap property, which is suitable for photonics application. Moreover, the band gap of dilute-As GaNAs alloy decreases as As-content increases, and the energy gap covers from 1.9 eV up to 3.5 eV which corresponds to the entire visible spectrum. The characteristics of the effective masses of electrons, heavy holes, and light holes for dilute-As GaNAs alloy with As-content up to 6.25% were presented. The electronic properties of dilute-As GaNAs alloy indicate the feasibility of this material for potential application as active regions in light-emitting diodes and lasers. Other potential advantage from the use of dilute-As GaNAs alloy may include the modification of the interband Auger recombination rate.

Acknowledgement: The authors acknowledge supports from National Science Foundation (Grant No. ECCS#0701421), US Department of Energy (Grant No. DE-FC26-08NT01581), and P. C. Rossin Professorship Funds.

REFERENCES

[1] Arif, R. A., Ee, Y. K., and Tansu, N., "Polarization Engineering via Staggered InGaN Quantum Wells for Radiative Efficiency Enhancement of Light Emitting Diodes Emitting," Appl. Phys. Lett., **91**, 091110 (2007).

[2] Arif, R. A., Zhao, H., and Tansu, N., "Spontaneous Emission and Characteristics of Staggered InGaN Quantum-Well Light-Emitting Diodes", IEEE J. Quantum Electron., **44**, 573 (2008).

[3] Arif, R. A., Ee, Y. K., and Tansu, N., "Nanostructure Engineering of InGaN-Based Active Regions for Improved III-Nitride Gain Media Emitting at 420-550 nm," in Physica Stat. Solidi (A), **205**, 96 (2008).

[4] Zhao, H., Arif, R. A., and Tansu, N., "Design Analysis of Staggered InGaN Quantum Wells Light-Emitting Diodes at 500-540 nm," *IEEE J. Sel. Top. in Quantum Electron.*, **15**, 1104 (2009).

[5] Zhao, H., Liu, G., Li, X. H., Huang, G. S., Poplawsky, J. D., Tafon Penn, S., Dierolf, V., and Tansu, N., "Growths of Staggered InGaN Quantum Wells Light-Emitting Diodes Emitting at 520-525 nm Employing Graded Growth-Temperature Profile," Appl. Phys. Lett., **95**, 061104 (2009).

[6] Zhao, H., Liu, G., Li, X. H., Arif, R. A., Huang, G. S., Poplawsky, J. D., Tafon Penn, S., Dierolf, V., and Tansu, N., "Design and Characteristics of Staggered InGaN Quantum Well Light-Emitting Diodes in the Green Spectral Regimes," IET Optoelectronics, **3**, 283 (2009).

[7] Zhao, H., Arif, R. A., Ee, Y. K., and Tansu, N., "Optical gain analysis of strain-compensated InGaN-AlGaN quantum well active regions for lasers emitting at 420–500 nm," Opt. Quantum Electron., **40**, 301 (2008).

[8] Zhao, H., Arif, R. A., Ee, Y. K., and Tansu, N., "Self-Consistent Analysis of Strain-Compensated InGaN–AlGaN Quantum Wells for Lasers and Light-Emitting Diodes," IEEE J. Quantum Electron., **45**, 66 (2009).

[9] Ee, Y. K., Arif, R. A., Tansu, N., Kumnorkaew, P., and Gilchrist, J. F., "Enhancement of Light Extraction Efficiency of InGaN Quantum Wells Light Emitting Diodes Using SiO_2 / Polystyrene Microlens Arrays," *Appl. Phys. Lett.*, **91**, 221107 (2007).

[10] Ee, Y. K., Kumnorkaew, P., Arif, R. A., Tong, H., Zhao, H., Gilchrist, J. F., and Tansu, N., "Optimization of Light Extraction Efficiency of III-Nitride Light Emitting Diodes with Self-Assembled Colloidal-based Microlenses," *IEEE J. Sel. Top. in Quantum Electron.*, **15**, 1218 (2009).

[11] Ee, Y. K., Kumnorkaew, P., Arif, R. A., Tong, H., Gilchrist, J. F., and Tansu, N., "Light Extraction Efficiency Enhancement of InGaN Quantum Wells Light-Emitting Diodes with Polydimethylsiloxane Concave Microstructures," *Optics Expres*s, **17**, 13747 (2009).

[12] Ee, Y. K., Biser, J. M., Cao, W., Chan, H. M., Vinci, R. P., and Tansu, N., "Metalorganic Vapor Phase Epitaxy of III-Nitride Light-Emitting Diodes on Nano-Patterned AGOG Sapphire Substrate by Abbreviated Growth Mode," *IEEE J. Sel. Top. Quantum Electron.*, **15**, 1066 (2009).

[13] Tansu, N, Kirsch, N. J., and Mawst, L. J., ""Low-Threshold-Current-Density 1300-nm Dilute-Nitride Quantum Well Lasers," Appl. Phys. Lett., 81, 2523 (2002).

[14] Lindsay, A. and O'Reilly, E. P., "Unification of the Band Anticrossing and Cluster-State Models of Dilute Nitride Semiconductor Alloys", Phys. Rev. Lett. 93, 196402 (2004)

[15] Tixier, S., Adamcyk, M., Young, E. C., Schmid, J. H., Tiedje, T., "Surfactant enhanced growth of GaNAs and InGaNAs using bismuth", J. Crystal Growth, vol 251, issue 1-4 (2003)

[16] Kudrawiec, R. et al, "Localized and delocalized states in GaNAs studied by microphotoluminescence and photoreflectance", Appl. Phys. Lett. 94, 011907 (2009)

[17] Tansu, N., Yeh, J. Y., and Mawst, L. J., "Physics and Characteristics of 1200-nm InGaAs and 1300-1400 nm InGaAsN Quantum-Well Lasers by Metalorganic Chemical Vapor Deposition," *Journal of Physics: Condensed Matter*, 16, S3277 (2004).

[18] Tansu, N., Yeh, J. Y., and Mawst, L. J., "Improved Photoluminescence of InGaAsN-(In)GaAsP Quantum Well by Organometallic Vapor Phase Epitaxy Using Growth Pause Annealing," *Appl. Phys. Lett.,* 82, 3008 (2003).

[19] Tansu, N., and Mawst, L. J., "Design Analysis of 1550-nm GaAsSb-(In)GaAsN Type-II Quantum Well Laser Active Regions," *IEEE J. Quantum Electron.*, 39, 1205 (2003).

[20] Vurgaftman, I., Meyer, J. R., Tansu, N., and Mawst, L. J., "InP-Based Dilute-Nitride Mid-Infrared Type-II "W" Quantum-Well Lasers," *J. Appl. Phys.*, 96, 4653 (2004).

[21] Tansu, N., and Mawst, L. J., "Current Injection Efficiency of 1300-nm InGaAsN Quantum-Well Lasers," *J. Appl. Phys*., 97, 054502 (2005).

[22] Thranhardt, A., Kuznetsova, I., Schlichenmaier, C., Koch, S. W., Shterengas, L., Belenky, G., Yeh, J. Y., Mawst, L. J., Tansu, N., Hader, J., Moloney, J. V., and Chow, W. W., "Nitrogen Incorporation Effects on Gain Properties in GaInNAs Lasers: Experiment and Theory," *Appl. Phys. Lett.*, 86, 201117 (2005).

[23] Palmer, D. J., Smowton, P. M., Blood, P., Yeh, J. Y., Mawst, L. J., and Tansu, N., "Effect of Nitrogen on Gain and Efficiency in InGaAsN Quantum Well Lasers", *Appl. Phys. Lett.,* 86, 071121 (2005).

[24] Tansu, N., Yeh, J. Y., and Mawst, L. J., "Experimental Evidence of Carrier Leakage in InGaAsN Quantum Well Lasers," Appl. Phys. Lett., 83, 2112 (2003).

[25] Wu, J., Walukiewicz, W., Yu, K. M., Denlinger, J. D., Shan, W., Ager III, J. W., Kimura, A., Tang, H. F., and Kuech, T. F., "Valence band hybridization in N-rich $GaN_{1-x}As_x$ alloys", Phys. Rev. B 70, 115214 (2004)

[26] Arif, R. A., Zhao, H., and Tansu, N, "Type-II InGaN-GaNAs quantum wells for lasers applications",Appl. Phys. Lett. 92, 062801 (2008).

[27] Zhao, H., Arif, R. A., and Tansu, N., "Self-consistent gain analysis of type-II 'W' InGaN–GaNAs quantum well lasers",J. Appl. Phys., 104, 043104 (2008).

[28] Kohn, W., and Sham, L. J., "Self-Consistent Equations Including Exchange and Correlation Effects", Phys. Rev. 140, A1133 (1965)

[29] Delaney, K. T. , Rinke, P., and Van de Walle, C. G., "Auger recombination rates in nitrides from first principles", Appl. Phys. Lett., 94, 191109 (2009)

[30] Van de Walle C. G., Neugebauer, J., "First-principles calculations for defects and impurities: Applications to III-nitrides", J. Appl. Phys. 95, 3851 (2004)

[31] Messmer, R. P. and Watkins, G. D., "in Radiation Damage and Defects in Semiconductors", Institute of Physics and Physical Society, London, No. 16, p. 255 (1972).

[32] Louie, S. G., Schluter, M., and Chelikowsky, J. R., "Self-consistent electronic states for reconstructed Si vacancy models", Phys. Rev. B 13, 1654 (1976).

[33] Pickett, W. E., Cohen, M. L., and Kittel, C., "Theory of the hydrogen interstitial impurity in germanium", Phys. Rev. B 20, 5050 (1979).

[34] Van de Walle, C. G., Denteneer, P. J. H., Bar-Yam, Y., and Pantelides, S. T., "Theory of hydrogen diffusion and reactions in crystalline silicon", Phys. Rev. B 39, 10 791 (1989).

[35] Broyden, C. G., "The Convergence of a Class of Double-rank Minimization Algorithms", J. of the Inst. of Math. & Its Appl.1970, 6, 76-90.

[36] Vurgaftman, I. and Meyer, J. R., "Band parameters for nitrogen-containing semiconductors", J. Appl. Phys. 94, 3675 (2003).